Available online at www.sciencedirect.com
ScienceDirect
Mendeleev Commun., 2016, **26**, 298–300
Mendeleev Communications

Surface modification of PtPd alloy electrodes by potential cycling: effect on electrocatalytic properties

Tatyana D. Gladysheva, Boris I. Podlovchenko,* Dmitry S. Volkov and Alexander Yu. Filatov

Department of Chemistry, M. V. Lomonosov Moscow State University, 119991 Moscow, Russian Federation. Fax: +7 495 939 0171; e-mail: podlov@elch.chem.msu.ru

DOI: 10.1016/j.mencom.2016.07.010

Cycling of the potential of the electrodeposit PtPd electrode causes a considerable increase in its activity in methanol oxidation.

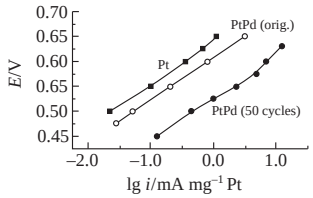

In the context of search for efficient electrocatalysts of methanol oxidation reaction (MOR) and formic acid oxidation reaction (FAOR), keen attention is drawn to mixed deposits of Pt and Pd.[1–10] Furthermore, both the deposits of volume mixtures[1–3,8] and core–shell structures[4–7,9,10] are studied. It should be noted that the last term is often used not only for Pt–Pd deposits with dense shells of Pt or Pd but also for structures with only the predominant presence of one component in the surface layer. According to the literature data,[1–10] the mixed Pt–Pd catalysts have the activity often close to that of monocomponent catalysts and even higher. From the practical viewpoint, the interest in Pt–Pd composites is largely associated with the necessity of decreasing the Pt content in catalysts for fuel cells.

The electrodeposits (e.d.) of platinum metals synthesized without use of any structure-forming organic compounds represent convenient model systems for studying highly dispersed catalysts. In our previous studies[9,10] ultra-small amounts of Pd[9] or Pt[10] were deposited on e.d. Pt and e.d. Pd, respectively, by the method of galvanic displacement (GD). The electrocatalytic properties of these composites were studied. In addition to the GD method, the method of electrochemical leaching (EL) can also be used for enriching the surface with one component of the binary system.[11–13] It was interesting to use the e.d. PtPd alloy as the basic Pt–Pd catalyst and investigate the possibility of synthesizing the core(PtPd)–shell(Pt) structure by leaching out the more easily dissolved component (Pd) from this alloy[14–17] by cycling its potential. Attention was focused on studying the changes in the composition and the surface characteristics of the composite and also in its activity in MOR and FAOR.

The deposition of the PtPd alloy on the glassy carbon (GC) support (S_{geom} = 1 cm^2) was carried out for ~40 min under potentiostatic conditions from a deaerated solution of 2.5×10^{-4} M H_2PtCl_4 + 2.5×10^{-4} M $PdCl_2$ + 0.5 M H_2SO_4 at E_{dep} = 0.25 V† on agitation with a magnetic stirrer (600 rpm). The deposition currents of Pt and Pd from their individual solutions 2.5×10^{-4} M H_2PtCl_4 and 2.5×10^{-4} M $PdCl_2$ at this potential were close to the diffusion current amounting to 0.25–0.3 mA cm^{-2}. If the partial currents of Pt and Pd deposition from mixed solutions remained the same as in individual solutions, the atomic ratio Pt : Pd should have been ~1 : 1; however, in the deposits obtained, the Pt content turned out to be much lower (see below), which pointed to substantial deviation from the diffusion mode of deposition. For a comparison, we used Pt/GC (1 mg Pt cm^{-2}) and Pd/GC (0.5 mg Pd cm^{-2}) synthesized under the same electrodeposition conditions. All freshly formed deposits were washed with the supporting electrolyte solution (0.5 M H_2SO_4), cathodically polarized to remove Cl^- ions, after which the electrochemically active surface area (EASA) was measured based on the currents of Cu_{ad} desorption.[9,18]

The deposits were subjected to leaching by cycling their potential in the range of 0.3–1.4 V at a scan rate of 13.3 mV s^{-1} in the supporting electrolyte solution. To control the kinetics of leaching, the solution was removed from the cell after every 10 cycles and analyzed for Pt and Pd. The cell was washed with the supporting electrolyte solution in an argon flow, a CVA was measured, and the cycling was resumed.

The total weight of e.d. PdPt was 0.65±0.05 mg. Table 1 shows a typical dependence of the amount of leached out Pd and Pt on the number of potential cycles in the interval involving the oxygen adsorption potentials. The adsorption–desorption of oxygen is known[14,15,17] to play the decisive role in the dissolution of platinum-group metals.

According to the literature data,[14,15] within its alloys too, palladium demonstrates the somewhat higher solubility as compared with platinum.

The fact that dissolution of Pt and Pd upon cycling of their alloy proceeds faster as compared with individual e.d. Pt/GC and e.d. Pd/GC attracts attention. This is an indirect indication that

Table 1 Amounts of Pt and Pd passed to solution upon cycling the electrode potential in the range of 0.3–1.4 V in 0.5 M H_2SO_4 (error ±10%).

Number of cycles	PtPd/GC		Pd/GC Pd/μg	Pt/GC Pt/μg
	Pd/μg	Pt/μg		
10	12.3	0.8	5.7	0.62
20	8.4	2.5	4.5	0.42
30	7.5	0.9	5.0	0.33
40	6.6	1.2	5.1	0.35
50	2.2	2.6	2.6	0.42
Total amount in 50 cycles	37.0	8.0	22.9	2.14

† Hereafter, all the potentials are shown with respect to the reversible hydrogen electrode in the same solution.

we observed the deposition of the alloy rather than that of the phases of its components.

The microprobe and AES-ICP analyses‡ of the composition of several original samples of e.d. PdPt gave their average atomic Pt : Pd ratio of 0.67±0.13. After 50 cycles, the bulk ratio of two metals did not change beyond the specified scatter of this value. This agrees with the tabulated data according to which the total mass of e.d. PtPd decreased by less than 8%. The XPS analysis accomplished on two original samples gave the Pt : Pd of 0.90–0.95 in the surface layer. A somewhat higher Pt content in the surface layers of the mixed e.d. sample as compared with its bulk composition was probably associated with the variation in the Pt : Pd ratio during the deposition.

The SEM images [Figure 1(*a*),(*b*)]‡ show that the shape and the size of conglomerates were different for Pd/GC (*a*) and Pt/GC (*b*). For Pt, the conglomerates had the shape close to spherical, whereas for Pd these conglomerates represented branched dendrites. On the surface of the PtPd/GC alloy [original sample (*c*)], as well as on the Pd/GC sample, the dendrites were present in a large amount. After cycling (50 cycles), the dendrites disappeared almost completely from the surface of PtPd/GC (*d*). One can assume that the dendrites of the alloy contained palladium in the amount at least much exceeding its average content in the deposit. However, the microprobe analysis in different points of the deposit [Figure 1(*c*)] has revealed that the bulk composition in regions filled with dendrites and those remote from them did not differ considerably. This points to sufficient homogeneity of the composition of PtPd particles of different shape.

Figure 2 shows CVA curves for PtPd/GC particles measured before and after the electrode potential cycling. Even in the initial curve of the mixed deposit (curve *1*), the initial part of the hydrogen region (from 60 mV) lacks the peak corresponding to the removal of the Pd(H) α,β-transition hydrogen[16,19] (*cf.* curve *1* for Pd/GC in the insert). According to ref. 16, the hydrogen dissolution in PtPd alloys practically stops at Pt : Pd (at.) > 0.35; however, the authors of the cited work accepted the possibility of

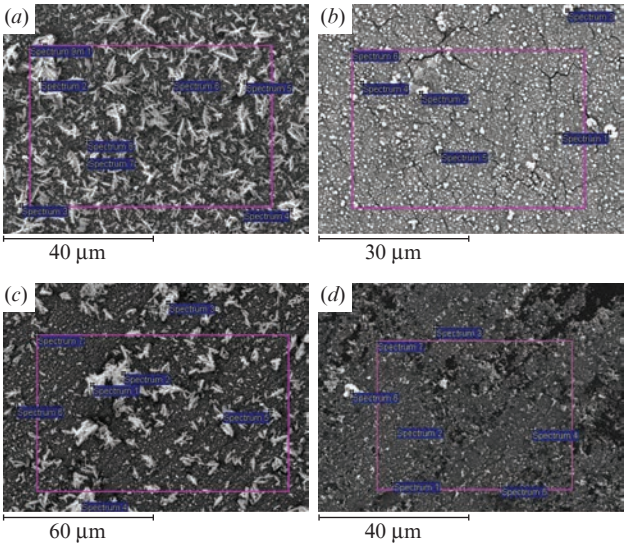

Figure 1 SEM images for (*a*) Pd/GC, (*b*) Pt/GC, (*c*) PtPd/GC (original), (*d*) PtPd/GC (after 50 cycles).

‡ The surface morphology of samples was studied by means of a scanning electron microscope JEOL JSM-6490 LV. The chemical composition in the bulk was determined by microprobe analysis and the AES-ICP method; the surface layer composition was analyzed by the XPS method.[9,10] The electrocatalytic activity was tested based on stationary currents of MOR (0.5 M MeOH + 0.5 M H_2SO_4) and FAOR (1 M HCOOH + 0.5 M H_2SO_4).[9,10] All the measurements were carried out at room temperature (20±1 °C).

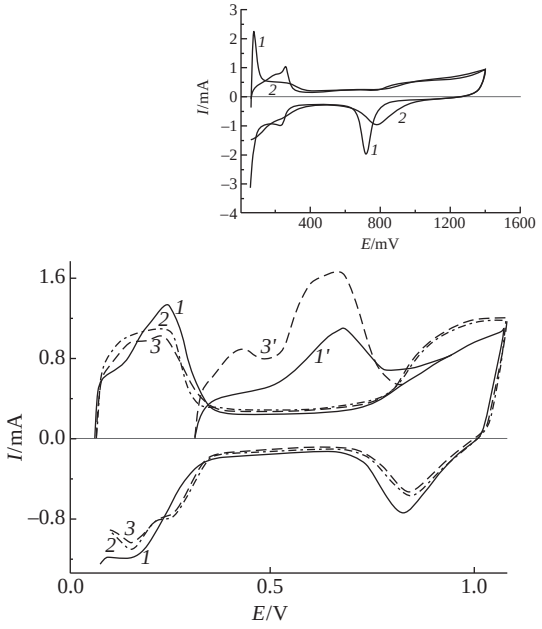

Figure 2 CVA curves in 0.5 M H_2SO_4 for PtPd/GC: (*1*) original deposit, (*2*) after 30 cycles, (*3*) after 50 cycles. Potentiodynamic curves of electrodesorption of Cu_{ad}: (*1′*) original deposit, (*3′*) after 50 cycles. Insert: CVA curves in 0.5 M H_2SO_4 for (*1*) Pd/GC, (*2*) Pt/GC. 6.6 mV s^{-1}.

the presence of microamounts of dissolved α-phase hydrogen. The potential cycling [curves *2*, *3*, Figure 2(*a*)] made the shape of curves in the hydrogen region closer to that of the curve for Pt/GC (Figure 2, curve *2* in insert). The cathodic branches of CVA for PtPd deposits demonstrated only one peak of adsorbed oxygen desorption, which was symmetrical. This undeniably points to the formation of the solid solution PtPd.[16,20]

An estimation based on the charges Q_{Cu} consumed in ionization of Cu_{ad} (Figure 2, curves *1′* and *3′*) gave the EASA values of 70–80, 70, and 40 cm^2 for the original PtPd/GC, Pt/GC, and Pd/GC, respectively. The specific values of EASA were approximately 13, 7, and 8 m^2 g^{-1} for PtPd/GC, Pt/GC, and Pd/GC, respectively. It should be stressed that for PtPd deposits, the total surface determined according to Q_{Cu} includes the surface atoms of both Pt and Pd.[9,10] Assessment of the average size of crystals *d* in terms of the model of spheres produced the values of ~25, 40, and 63 nm for e.d. PtPd, e.d. Pt, and e.d. Pd, respectively. To calculate *d*, one has to know the deposit density. For e.d. PtPd, the latter was assumed to be 18.3 g cm^{-3} according to the equation for mixed solutions: DM = XA·DA + XB·DB, where DM is the mixture density, XA and XB are the volume fractions of components A and B (it was assumed that Pt : Pd = 0.7), DA and DB are the densities of A and B (Pt 21.5 g cm^{-3}, Pd 11.9 g cm^{-3}). As seen, the PtPd deposits were characterized by the higher degree of dispersion as compared with e.d. Pd and e.d. Pt. This can be one of the reasons for the higher solubility of the mixed deposit as compared with individual Pt and Pd deposits.

The value of EASA for PtPd/GC electrodes increased as a result of electrode potential cycling (compare curves *1′* and *3′*, Figure 2) and after 50 cycles exceeded the initial values by a factor of 1.3–1.5 (for different samples). This growth can be associated with the increase in the number of micropores in the deposit.[21] The variation in the $Q_H/0.5Q_{Cu}$ ratio was analyzed (when assessing the amount of adsorbed hydrogen in the charges Q_H, the hydrogen and double layer regions of anodic branches of CVA were extrapolated to $E = 0$). For the initial PtPd/GC samples, this ratio was ~2; after 50 cycles it became ~1 (for Pt/GC, $Q_H/0.5Q_{Cu} \approx 1$; for Pd/GC, $Q_H/0.5Q_{Cu} \approx 3$). It can be assumed that in the initial samples of e.d. PtPd, the absorption of hydrogen in the PtPd(H) α-phase was present. After 50 cycles, virtually no

hydrogen dissolution was observed, although the Pd content in the bulk did not change significantly. This allowed us to suppose that the number of defects in the deposit bulk decreased with cycling.[19]

Assuming that the number of atoms in 1 cm^2 of the Pd monolayer (ML) is 1.3×10^{15} (the mass equivalent is 0.23 μg cm^{-2}) and the mass of Pd dissolved in 50 cycles is 31 μg (see Table 1), we obtain that ~135 cm^2 of MLPd was dissolved in one experiment. This value is more than twice as high as the average EASA value of the original mixed deposit, which allows us to believe that the leaching process penetrated only a little into the grains and no platinum shells were formed. The latter was confirmed by the XPS data demonstrating that the surface layer became enriched with platinum during the cycling (Pt : Pd is 1.30–1.45), however, a considerable amount (~40 at%) of Pd was retained. The binding energy of Pt[$4f_{7/2}$] electrons is 71.0 eV, which is close to the binding energy of metal platinum (71.2 eV). The somewhat lower energy value can be associated with the interaction of platinum with palladium.

The specific activity in FAOR for the mixed PtPd deposit (Figure 3, curve *1*) was somewhat higher than the activity of e.d. Pt (curve *3*) but much lower than that of Pd/GC (curve *4*). As a result of cycling which increased the Pt content in the surface layer, the activity decreased further (Figure 3, curve *2*) approaching that of Pt/GC (curve *3*). These results are not unexpected because it is well known that Pt is the much less active catalyst of FAOR as compared with Pd.

The more interesting data were obtained for MOR. The specific surface activity of the original PtPd deposit in MOR [Figure 4(*a*), curve *1*] was already somewhat higher than the activity of e.d. Pt (curve *3*) and increased during electrode potential cycling (curve *2*). The current of the modified electrode exceeded the current on e.d. Pt by a factor of ~5. In our previous studies,[9,10] in which the Pt and Pd clusters were deposited on the phase deposits of Pd and Pt, respectively, we observed no promoting effect of the added component on the composite activity. This allows us to conclude that the promoting effect is intrinsic of the solid solution PtPd. The higher specific activity in MOR of the dendrites of the PtPd alloy as compared with disperse Pt was also mentioned.[8]

On the surface of a solid solution the effect of the 'third body'[22] probably occurs: the presence of palladium atoms in the first monolayer reduced the number of platforms, on which strong many-places chemisorption of products of electrooxidation of methanol can proceed. The latter, as we know, inhibits MOR. Changes in the activity to a certain extent can be associated with changes in the structure of deposit. Cycling of the potential of e.d. PtPd gives rise not only to the enrichment of the surface layer with platinum but also to the substantial change in its structure. According to published data,[23] in which the specific activities of e.d. Pt and smooth Pt were compared, the activity of polycrystalline Pt in MOR can change by a factor of 3–4 due to the structural reasons.

The stationary currents calculated per the Pt mass in the catalyst are of the greater interest for practice because characterize the level of Pt utilization. Figure 4(*b*) shows that after the current was recalculated from mA cm^{-2} to mA mg^{-1}Pt, the higher activity of the modified PtPd/GC electrode as compared with Pt/GC electrode became even more pronounced. At 550 mV, the specific mass activity of cycled PtPd/GC exceeded that of the Pt/GC electrode by a factor of ~10.

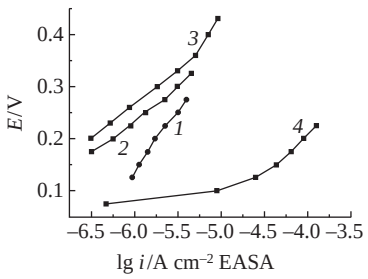

Figure 3 Stationary polarization curves of FAOR in solution 1 M HCOOH + + 0.5 M H_2SO_4: (*1*) PtPd/GC original deposit, (*2*) PtPd/GC after 50 cycles, (*3*) Pt/GC, (*4*) Pd/GC.

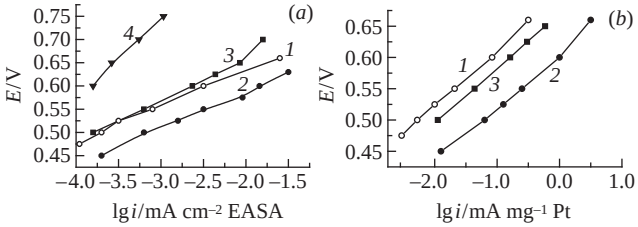

Figure 4 Stationary polarization curves of MOR in solution 0.5 M MeOH + + 0.5 M H_2SO_4, normalized to (*a*) EASA and (*b*) Pt mass: (*1*) PtPd/GC original deposit, (*2*) PtPd/GC after 50 cycles, (*3*) Pt/GC, (*4*) Pd/GC.

Summarizing, we can regard the following results as the most significant: (i) a considerable promoting effect of potential cycling on the activity of the electrodeposited PtPd alloy in MOR was revealed and (ii) the higher solubility of Pt and Pd from their alloy as compared with individual e.d. Pt and e.d. Pd was established.

The study was supported by the Russian Foundation for Basic Research (project no. 15-03-03436) and in part within the framework of the M. V. Lomonosov Moscow State University Program of Development.

References

1 A. Capon and R. Parsons, *J. Electroanal. Chem.*, 1975, **65**, 285.
2 L. Wang, Y. Nemoto and Y. Yamauchi, *J. Am. Chem. Soc.*, 2011, **133**, 9674.
3 F. Kadirgan, S. Beyhan and T. Atilan, *Int. J. Hydrogen Energy*, 2009, **34**, 4312.
4 K. Sasaki, H. Naohara, Y. Cai, Y. M. Choi, P. Liu, M. B. Vukmirovic, J. X. Wang and R. R. Adzic, *Angew. Chem. Int. Ed.*, 2010, **49**, 8602.
5 N. V. Long, M. Ohtaki, T. D. Hien, J. Randy and M. Nogami, *Electrochim. Acta*, 2011, **56**, 9133.
6 R. Huang, Y.-H. Wen, Z.-Z. Zhu and S.-G. Sun, *J. Phys. Chem. C*, 2012, **116**, 8664.
7 M. Liao, Y. Wang, G. Chen, H. Zhou, Y. Li, C.-J. Zhong and B. H. Chen, *J. Power Sources*, 2014, **257**, 45.
8 Q. Wang, Y. Li, G. Xu, G. Zhang, Q. Zhau and J. Zhang, *J. Power Sources*, 2015, **297**, 5967.
9 T. D. Gladysheva, A. Yu. Filatov and B. I. Podlovchenko, *Mendeleev Commun.*, 2015, **25**, 56.
10 B. I. Podlovchenko, T. D. Gladysheva and A. Yu. Filatov, *Mendeleev Commun.*, 2015, **25**, 293.
11 N. Hodnik, M. Bele and S. Hočevar, *Electrochem. Commun.*, 2012, **23**, 125.
12 G. Saravanan, K. Nanba, G. Kabayashi and F. Matsumoto, *Electrochim. Acta*, 2013, **99**, 15.
13 B. I. Podlovchenko, Yu. M. Maksimov and A. G. Utkin, *Russ. J. Electrochem.*, 2015, **51**, 891 (*Elektrokhimiya*, 2015, **51**, 1011).
14 D. A. J. Rand and R. Woods, *J. Electroanal. Chem.*, 1972, **36**, 57.
15 M. Łukaszewski and A. Czerwiński, *J. Electroanal. Chem.*, 2006, **589**, 38.
16 M. Grdeń, A. Piaścik, Z. Koczorowski and A. Czerwiński, *J. Electroanal. Chem.*, 2002, **532**, 35.
17 Yu. M. Maksimov, A. V. Smolin and B. I. Podlovchenko, *Russ. J. Electrochem.*, 2007, **43**, 1412 (*Elektrokhimiya*, 2007, **43**, 1493).
18 Yu. M. Maksimov, A. S. Lapa and B. I. Podlovchenko, *Sov. Electrochem.*, 1989, **25**, 634 (*Elektrokhimiya*, 1989, **25**, 712).
19 B. I. Podlovchenko, E. A. Kolyadko and S. Lu, *J. Electroanal. Chem.*, 1995, **399**, 21.
20 G. A. Attard and A. Bannister, *J. Electroanal. Chem.*, 1991, **300**, 467.
21 T. D. Gladysheva, E. I. Shkolnikov, Yu. M. Volfkovich and B. I. Podlovchenko, *Elektrokhimiya*, 1982, **18**, 435 (in Russian).
22 H. Angerstein-Kozlowska, B. MacDougall and B. Conway, *J. Electrochem. Soc.*, 1973, **120**, 756.
23 B. I. Podlovchenko and R. P. Petukhova, *Elektrokhimiya*, 1972, **8**, 899 (in Russian).

Received: 25th January 2016; Com. 16/4823